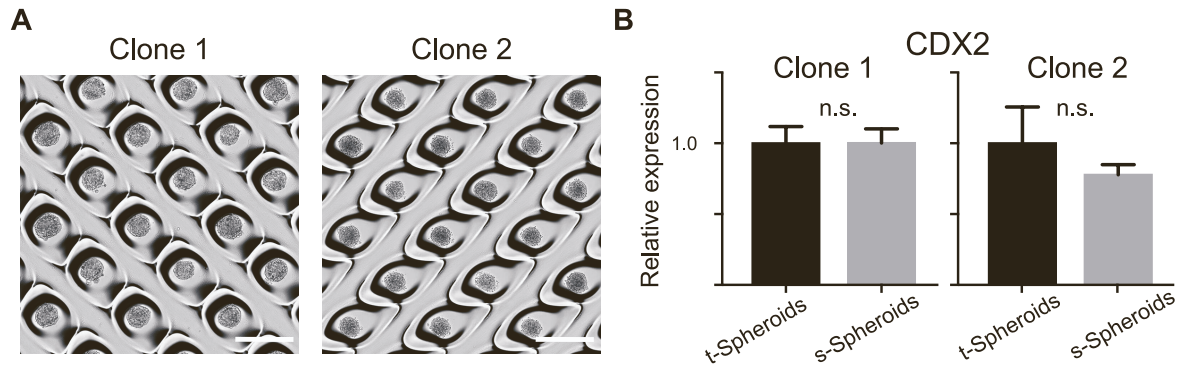


**Cell Reports Methods, Volume 2**

**Supplemental information**

**Suspension culture in a rotating bioreactor for  
efficient generation of human intestinal organoids**

**Junichi Takahashi, Tomohiro Mizutani, Hady Yuki Sugihara, Sayaka Nagata, Shu Kato, Yui Hiraguri, Sayaka Takeoka, Mao Tsuchiya, Reiko Kuno, Sei Kakinuma, Mamoru Watanabe, and Ryuichi Okamoto**



**Figure S1 Generation of homogeneous suspension spheroids (s-Spheroids) from multiple iPSC lines. Related to Figure 1.**

(A) Bright-field images of s-Spheroids differentiated from multiple iPSC lines using EZSPHERE 6-well plates. Scale bar, 500  $\mu\text{m}$ . (B) *CDX2* expression in formed t-Spheroids and s-Spheroids induced from two independent iPSC clones was analyzed by qRT-PCR. Data are means  $\pm$  s.d. for triplicate independent experiments. Unpaired, two-tailed *t*-test.

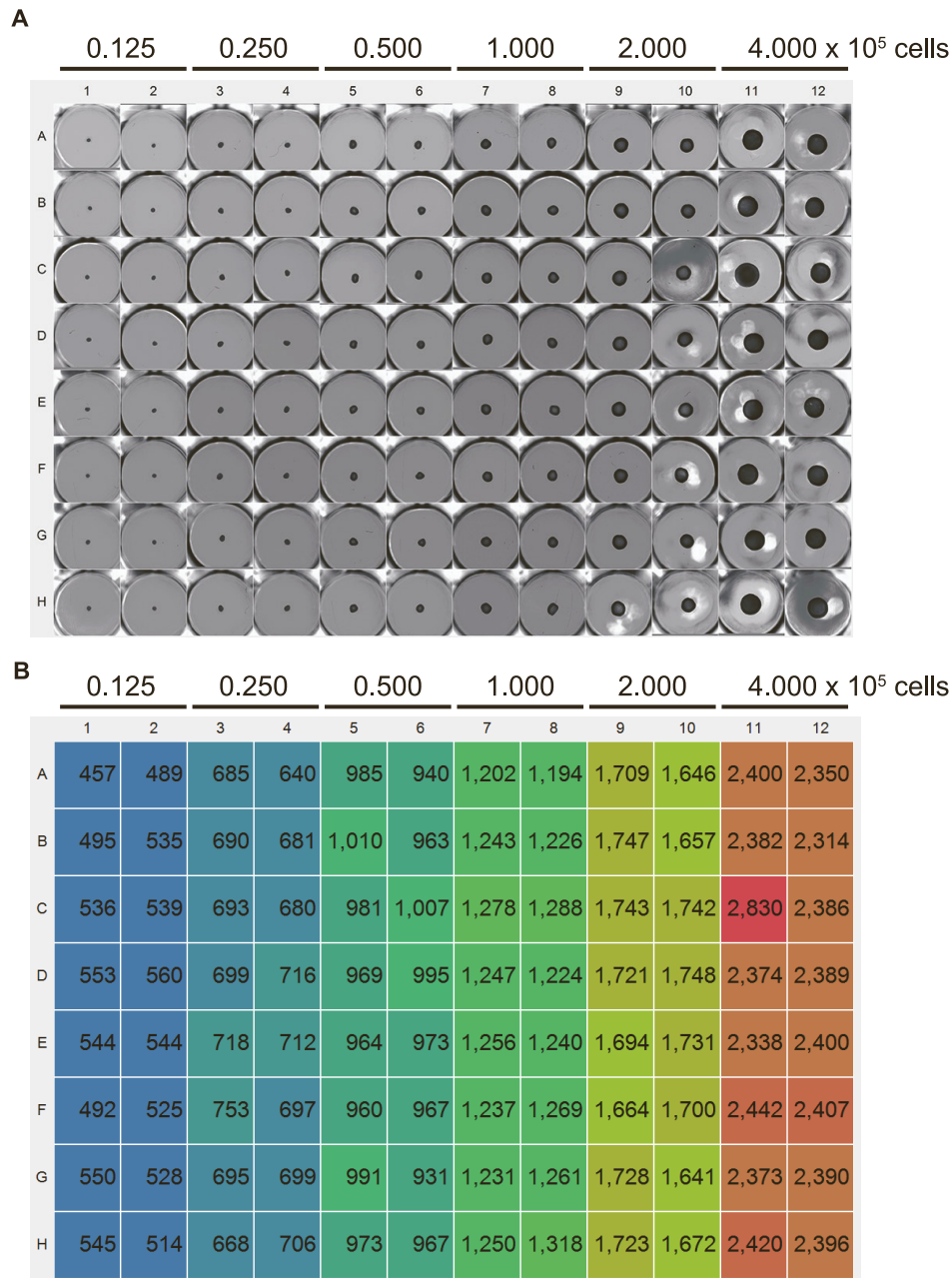


**Figure S2 Effect of starting cell number on the size of suspension spheroids generated by seeding cells onto spheroid forming plate. Related to Figure 2.**

A range of dissociated cells were seeded onto a 96-well spheroid forming plate (EZ-BindShut<sup>®</sup> SP 96-well plate) to create suspension spheroids. **(A)** Bright-field images of formed suspension hindgut spheroids on spheroid forming plate starting from 0.125 x 10<sup>5</sup> to 4 x 10<sup>5</sup> cells. Each cell number condition was performed in 16 independent wells. The diameter of spheroids after 24 hrs induction was analyzed by the bright-field imaging scanner, Cell<sup>3</sup> iMager duos. **(B)** Heat map of spheroid diameters (μm) in each condition was visualized with Cell<sup>3</sup> iMager duos Software Ver. 1.6 (SCREEN Holdings Co., Ltd., Kyoto, Japan).

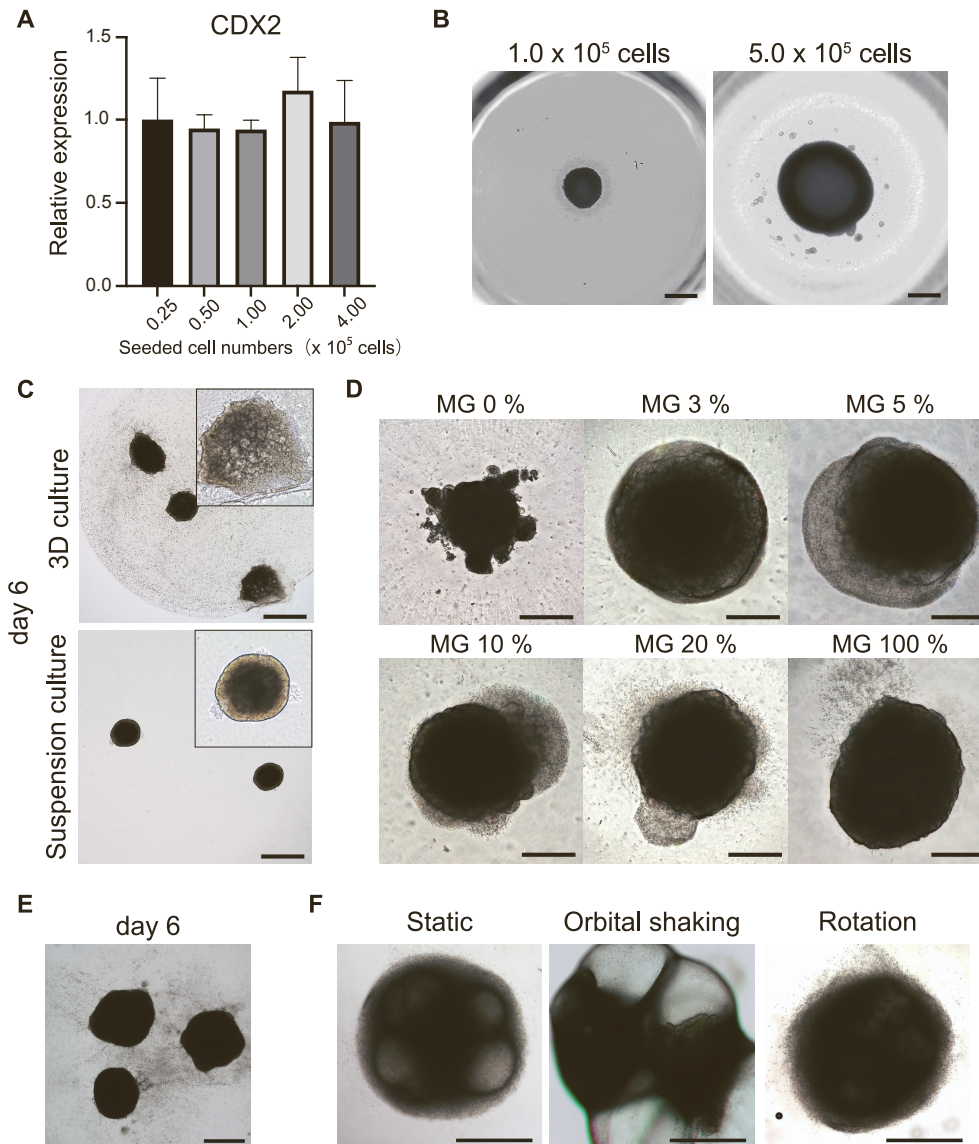


**Figure S3 Optimized conditions for suspension spheroid expansion. Related to Figures 2 and 3.**

(A) Expression of *CDX2* in s-Spheroids generated from different cell numbers was analyzed by qRT-PCR. Data are means  $\pm$  s.d. for quadruplicate independent experiments. Unpaired, two-tailed *t*-test. (B) s-Spheroids generated from  $1 \times 10^5$  cells are spherical, whereas s-Spheroids generated from  $5 \times 10^5$  cells are biconcave-disk-like as the lighter colored center illustrate thinner structure compared to the rim. Scale bar, 1000  $\mu\text{m}$ . (C) Bright-field images of s-Spheroids cultivated in the traditional three-dimensional culture (upper panel) and the suspension culture (lower panel). s-Spheroids easily attached to the bottom of the plate in three-dimensional culture. Scale bar, 1000  $\mu\text{m}$ . (D) Single spheroids were formed on the EZ-BindShut and cultured in suspension with the spheroid culture medium adding various concentrations of Matrigel (0 %, 3 %, 5 %, 10 %, 20 %, and 100 %) for 14 days. Light microscopy images of spheroids showed at least 3 % of Matrigel was needed to maintain suspension spheroids. Budding feature was observed in spheroids cultured in 10 % - 20 % Matrigel conditions. Scale bar, 500  $\mu\text{m}$ . (E) A bright-field image of dead large spheroids generated from  $1 \times 10^6$  cells in a static suspension culture. Scale bar, 1000  $\mu\text{m}$ . (F) Bright-field images of s-Spheroids cultured in suspension in a static (left), an orbital shaking (middle), and rotational bioreactor (right) condition. s-Spheroids cultured in an orbital shaker gather in the center and fuse. Scale bar, 1000  $\mu\text{m}$ .

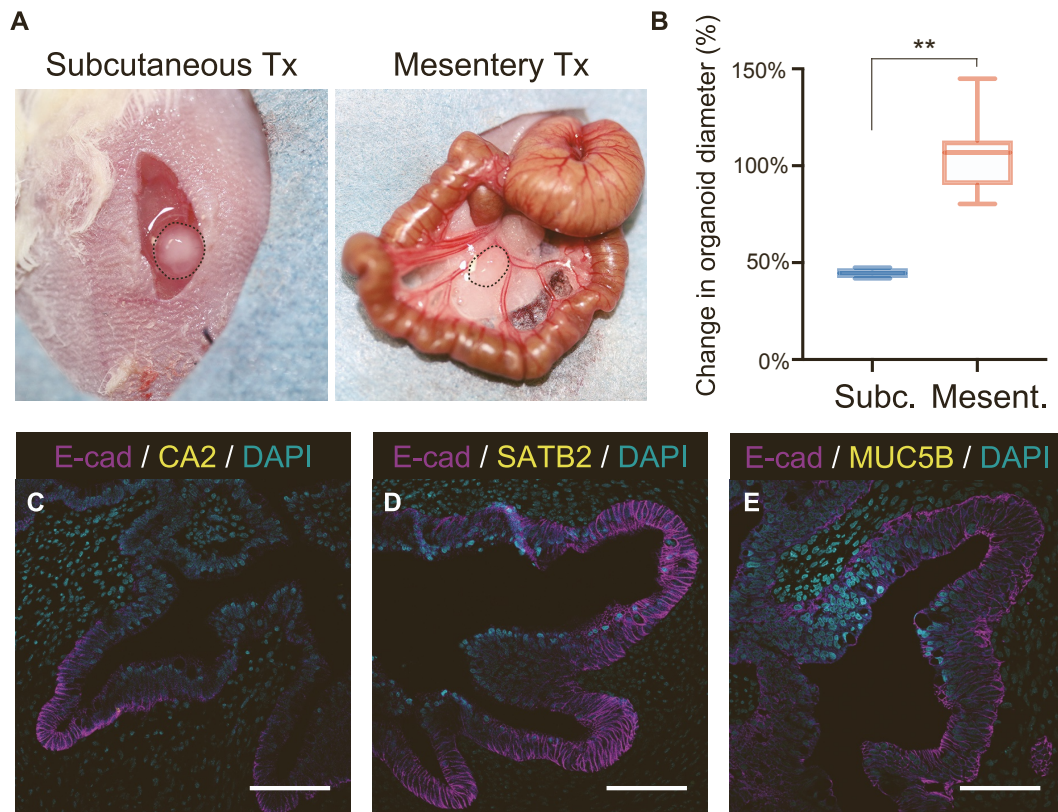


**Figure S4 Engrafted various-size s-HIOs show *in vivo* growth into small intestinal tissue. Related to Figure 4.**

Cultured s-HIOs matured from middle-sized s-spheroids were transplanted into the mesentery and subcutaneous lesion of NSG mice. **(A)** after 4 weeks of *in vivo* growth, the s-HIOs have engrafted into the mesentery (Mesentery Tx) and subcutaneous lesion (Subcutaneous Tx). The grafts are outlined in black. **(B)** s-HIOs engrafted into mesentery (Mesent.) grew larger than those engrafted into the subcutaneous region (Subc.) at the time of harvest (change in size =  $44.58\% \pm 2.514$  vs  $106.3\% \pm 20.77$ ,  $P < .0001$ ). **(C)-(E)** Immunostaining of engrafted intestinal HIOs revealing lack of colonic markers; carbonic anhydrase II (CA2), Special AT-rich sequence-binding protein 2 (SATB2), colonic type goblet cell marker MUC5B. Scale bar, 100  $\mu\text{m}$ .

**Table S1 List of growth factors. Related to Figure 2.**

<b>Factor</b>	<b>Final concentration</b>	<b>Epithelial growth</b>	<b>Mesenchymal growth</b>
<b>Wnt3a</b>	200 ng/ml	↑	↓
<b>CHIR99021</b>	3 $\mu$ M	↑	↓
<b>FGF-2</b>	50 ng/ml	↑	↑
<b>FGF-4</b>	50 ng/ml	↑	↑
<b>IGF-1</b>	100 ng/ml	→	→
<b>SB202190</b>	10 $\mu$ M	→	→
<b>A83-01</b>	500 nM	↑	→
<b>Nicotinamide</b>	10 mM	→	→
<b>Forskolin</b>	20 $\mu$ M	↑	↓